

Conjugated Carbonyl Polymer-Based Flexible Cathode for Superior Lithium–Organic Batteries

Qiang Li,[†] Dongni Li,[†] Haidong Wang,[†] Heng-guo Wang,^{*,†,‡} Yanhui Li,[†] Zhenjun Si,^{*,†} and Qian Duan^{*,†,‡}

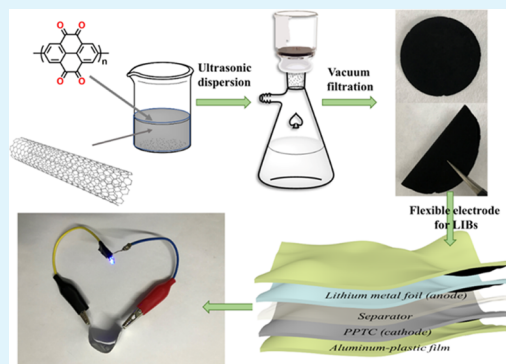
[†]School of Materials Science and Engineering, Changchun University of Science and Technology, Changchun 130022, China

[‡]Engineering Research Center of Optoelectronic Functional Materials, Ministry of Education, Changchun 130022, China

Supporting Information

ABSTRACT: Conjugated carbonyl compounds are deemed as high theoretical capacity and green electrode materials for lithium-ion batteries (LIBs) but are limited by their high dissolution and poor electronic conductivity. In this paper, we have successfully synthesized a series of multicarbonyl conjugated polymers using the coupling polymerization reaction and then constructed carbonyl-conjugated polymer/carbon nanotube hybrid films by a vacuum-filtration method. Importantly, the hybrid films could serve as a flexible, binder-free, and free-standing organic cathode for LIBs, which could deliver a high reversible discharge capacity of 142.3 mAh g⁻¹ at 50 mA g⁻¹, good cycling stability with a capacity retention of 74.6% at 500 mA g⁻¹ after 300 cycles, and excellent rate capability of 120.6 mAh g⁻¹ at 1000 mA g⁻¹. In addition, the theoretical calculation has proved that the symmetrical conjugated structure can well accommodate four Li⁺ ions during the electrochemical reaction. Interestingly, the assembled full cell and flexible battery can power the small devices, suggesting its potential to use in bendable or wearable energy-storages devices.

KEYWORDS: conjugated carbonyl polymer, organic cathode materials, flexible electrode, coupling polymerization, lithium-organic batteries



1. INTRODUCTION

Lithium-ion batteries (LIBs) have been emerged as the most promising energy storage devices for applying in smart grids, portable electronics, electric vehicles, and large-scale energy storage systems.^{1–3} However, the commercial LIBs are focused on inorganic electrode materials, which are almost obtained from nonrenewable mineral resources and their manufactures are often associated with huge energy cost and environment pollution. Furthermore, the intrinsic properties of inorganic materials would limit their specific capacities and cause safety problems.^{4–6} Thus, it is necessary to develop sustainable and environmentally friendly electrode materials to meet the growing demand of green energy.^{7–10}

Compared with those of inorganic materials, organic electrode materials have many overwhelming advantages, including high specific capacity, low cost, small environment pollution, and abundant resources.^{11–15} Until now, conjugated carbonyl organic compounds such as quinones,^{16,17} anhydrides,^{18,19} and ketones^{18,20} have been emerged as the most hopeful organic electrode materials because of their redox stability, structure diversity, multielectron reactions, and fast reaction kinetics.^{21,22} However, these organic compounds also show high dissolution in organic electrolytes, which results in fast capacity attenuation during cycling.^{23–26} From the perspective of molecular engineering, polymerization is a

valid strategy to suppress the dissolution problem.^{27,28} Generally, the formation of polymers is realized by combining electrochemical active monomer with some inactive linker groups, such as methylene,²³ imine,²² and thioether groups.²⁹ Although the dissolution problem of organic compounds could be greatly improved, the increase weight of inactive moieties will decrease their theoretical capacity. Therefore, using the cross-coupling method to directly construct C–C coupled conjugated carbonyl polymers without additional linker groups may be an ideal strategy to exploit high-performance organic electrode materials for LIBs. However, there still exists the inherent defect of poor electronic conductivity for organic materials. As a response, the incorporation of carbon materials, such as graphene and carbon nanotubes (CNTs), is an efficient tactic to improve the conductivity of organic active materials. Moreover, the carbon matrix endows organic compound-based composite materials with a flexible feature, which could be served as a free-standing electrode without using a binder, a conductive additive, and a metal current collector. This flexible electrode can not only simplify the manufacturing operation of the conventional electrodes but also enhance the battery

Received: April 12, 2019

Accepted: July 17, 2019

Published: July 17, 2019

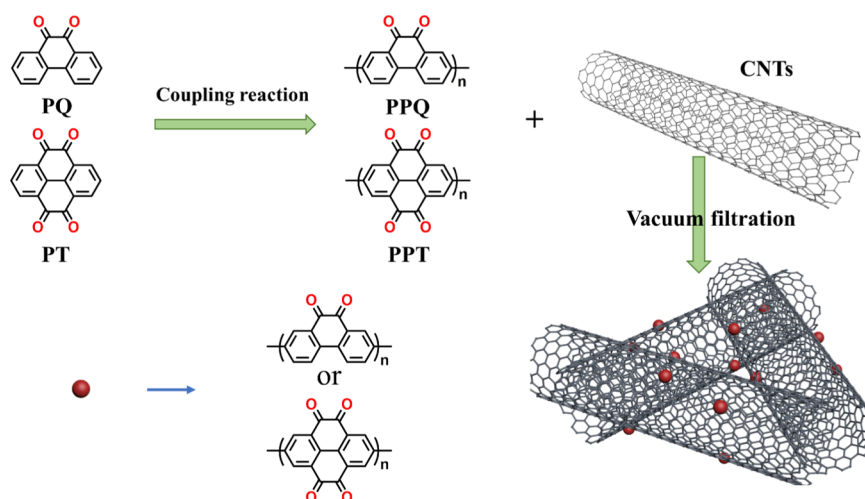


Figure 1. Schematic of the synthesis route for the PPT/PPQ-based flexible and free-standing film.

performance including the increased energy/power densities and the enhanced safety problems, which can promote the rapid expansion of flexible electronic devices.^{30,31} Therefore, it is imperative to construct C–C coupled conjugated carbonyl polymer-based free-standing and flexible electrode for efficient lithium-organic batteries.

Herein, we have successfully synthesized a series of conjugated carbonyl polymers by a one-step organometallic polycondensation reaction and then constructed flexible and free-standing conjugated carbonyl polymer/CNT hybrid films (PPTC) through the easy vacuum-filtration method. Two types of conjugated carbonyl polymers, including poly(pyrene-4,5,9,10-tetraone) (PPT) and poly(9,10-phenanthrenequinone) (PPQ), were synthesized using the cross-coupling method without additional inactive linker groups, which avoids the increase of molecular weight and extends the conjugated structure of molecule, thus showing a higher capacity and reduction potential. Furthermore, the incorporation of CNTs endows the hybrid films with a flexible feature, which could be served as a flexible, binder-free, and free-standing organic electrode for LIBs. To study the effect of Li coordination on the chemical structure, the energy levels and electronic distribution of lithiated PT and PQ are also calculated by density functional theory (DFT). As a result, a hybrid flexible electrode consisting of PPT with four carbonyl groups (PPTC) shows superior electrochemical performance compared to that of PPQ with two carbonyl groups (PPQC).

2. EXPERIMENTAL SECTION

2.1. Synthesis of Poly(pyrene-4,5,9,10-tetraone) (PPT). PPTs were synthesized according to the reported method.^{32,33} First, Ni(COD)₂ (2 mmol, 550 mg), bipyridine (BPY, 2 mmol, 312 mg), and 1,5-cyclooctadiene (COD, 1.5 mmol, 135 μ L) were dissolved in 20 mL of dimethylformamide (DMF). Then, the solution containing PT-2Br (1.5 mmol, 633 mg) and 10 mL of DMF was added into the above solution dropwise. All of the above experiments were operated in a N₂-filled glovebox. Finally, the assembled reactor was sealed and kept at 60 °C for 7 days. After the reaction, the solution was poured into a 50 mL mixture of diluted HCl (1 M) and methanol (1:1, v/v) and then the deep brown precipitate was filtrated and washed with 1 M HCl, H₂O, and methanol. Finally, the products were further purified by dissolving in DMF and recrystallized by injecting methanol.

2.2. Preparation of the Flexible and Free-Standing Film. To fabricate a PPT-based flexible and free-standing film, the PPT and

CNTs were first dispersed into ethanol (20 mL) and then the mixture was sonicated for 2 h to form a uniform suspension. Finally, the suspension was loaded on a microfiltration membrane (0.22 μ m poly(vinylidene fluoride) microporous membrane) through a vacuum filter. After drying at 70 °C under vacuum, a flexible and self-standing film was obtained. Herein, different samples were prepared by adjusting different mass ratios of polymers to CNTs (1:1, 1:2, and 1:3), which were denoted PPTC-1, PPTC, and PPTC-3. For comparison, the PQ-based film was prepared by the same method, which was denoted PPQC. In addition, the bare CNT electrode was directly prepared through a vacuum filter without adding active materials.

2.3. Electrochemical Characterization. The electrochemical performance was examined using CR2025 coin half-cells that contain lithium foil as an anode, a Celgard 2400 membrane as separator, 1 M LiTFSI dissolved in a mixed solvent of 1,3-dioxolane and dimethoxyethane (1:1, vol %) as an electrolyte, and the binder-free and free-standing films as a cathode (the electrodes were cut into disks with a diameter of 12 mm and the mass loading of 0.49–0.73 mg cm⁻² of the active material). For comparison, the traditional working electrodes were composed of active material, acetylene black, and poly(vinylidene fluoride) (3:6:1 or 8:1:1). The slurry was grinded over 1 h by adding NMP as the solvent, which was then uniformly adhered onto the Al foil and dried at 70 °C for 24 h. All of the batteries were assembled in an argon-filled glovebox.

3. RESULTS AND DISCUSSION

The synthetic process of the PPT/PPQ-based flexible films is schematically shown in Figure 1. First, the symmetrical/asymmetrical conjugated carbonyl compounds of PT/PQ with four/two carbonyl groups are chosen as the unique structural unit of polymerization due to their conjugated structure and high theoretical capacity (409/260 mAh g⁻¹). In fact, organometallic polycondensation based on the C–C coupling reaction, e.g., Ni(0) complex catalyzes dehalogenation polycondensation reactions of dihaloaromatic compounds $nX-Ar-X + nNiL_m \rightarrow -(Ar)_n- + nNiX_2L_m$, where X represents a halogen, L represents a ligand, and Ar represents an aromatic ring, has been demonstrated as an effective method to directly prepare conjugated polymers.^{32–35} Herein, two types of conjugated carbonyl polymers are synthesized using the C–C coupling reaction catalyzed by Ni(COD)₂ as the catalyst (detailed synthesis and characterization of these compounds are shown in the Supporting Information). Subsequently, the as-prepared PPT/PPQ is mixed with the CNTs by sonication and then the easy vacuum-filtration

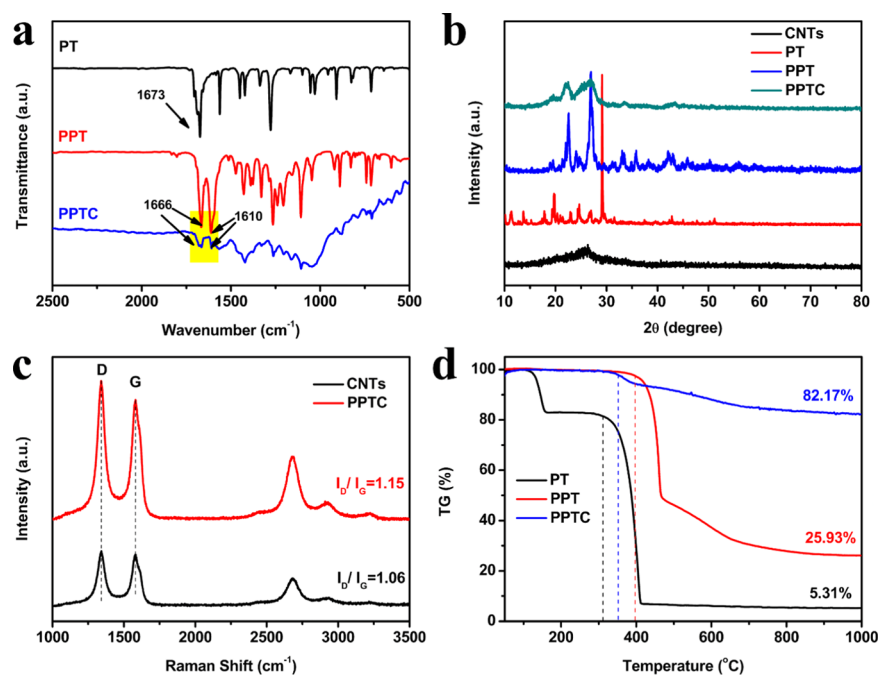


Figure 2. (a) FT-IR spectra and (b) XRD patterns of CNTs, PT, PPT, and PPTC. (c) Raman spectra of CNTs and PPTC. (d) Thermogravimetric curves of PT, PPT, and PPTC under a N_2 atmosphere.

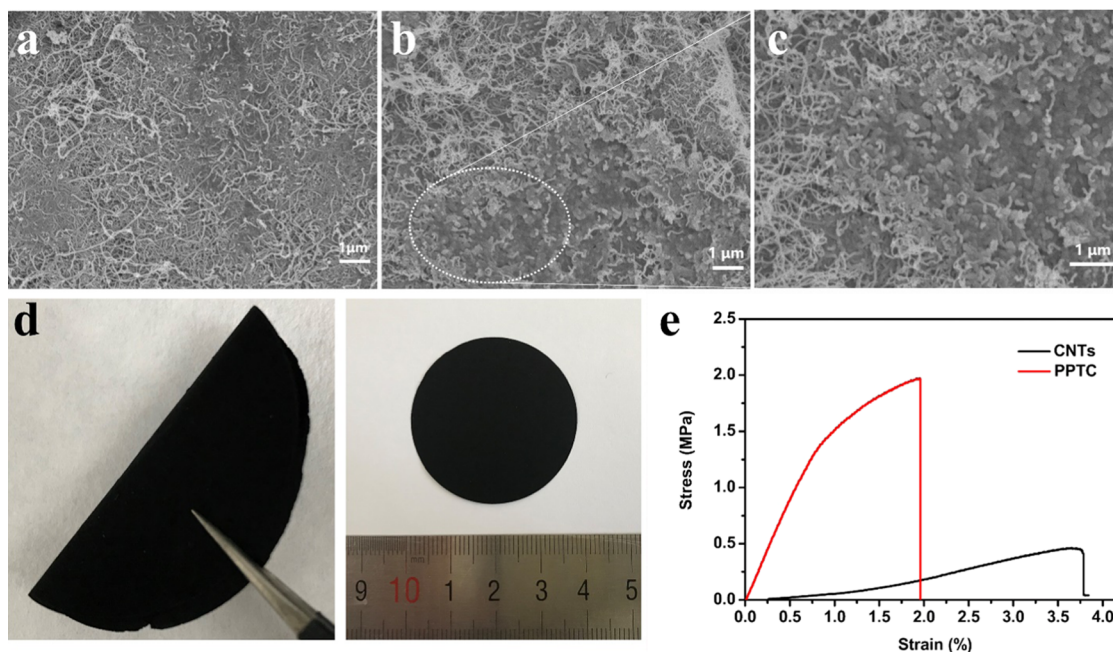


Figure 3. SEM images of (a) CNTs and (b, c) PPTC. (d) Photograph of the flexible free-standing PPTC film. (e) Stress–strain curves of CNTs and PPTC.

method is applied to construct the PPT/PPQ-based flexible film. Herein, the strong π - π interaction between conjugated carbonyl compounds and CNTs promotes the formation of a flexible film and further suppresses the dissolution of the conjugated carbonyl polymers.

The structures of various samples are first confirmed by 1H NMR and UV-vis absorption spectra (Figures S1–S5). Intuitively, the PPT and PPQ show insolubility compared to that of the monomers PT and PQ in different solvents (Figure S6), which confirm the formation of the polymers. Fourier transform infrared (FT-IR) spectroscopy is used to character-

ize the structure of various samples. In Figure 2a, the characteristic peaks for C=O and C=C of PPT show an obvious shift and become broader compared to those for PT monomer, indicating the formation of polymers. In addition, the existence of the peaks from the polymers in PPTC shows the formation of the hybrid films and the absence of spectral changes for PPT and PPTC indicates the noncovalent functionalization between PPT and CNTs. The change of the crystal structure is investigated by the X-ray diffraction (XRD) (Figure 2b). The existence of many sharp diffraction peaks manifest that PT has an obvious crystalline structure. In

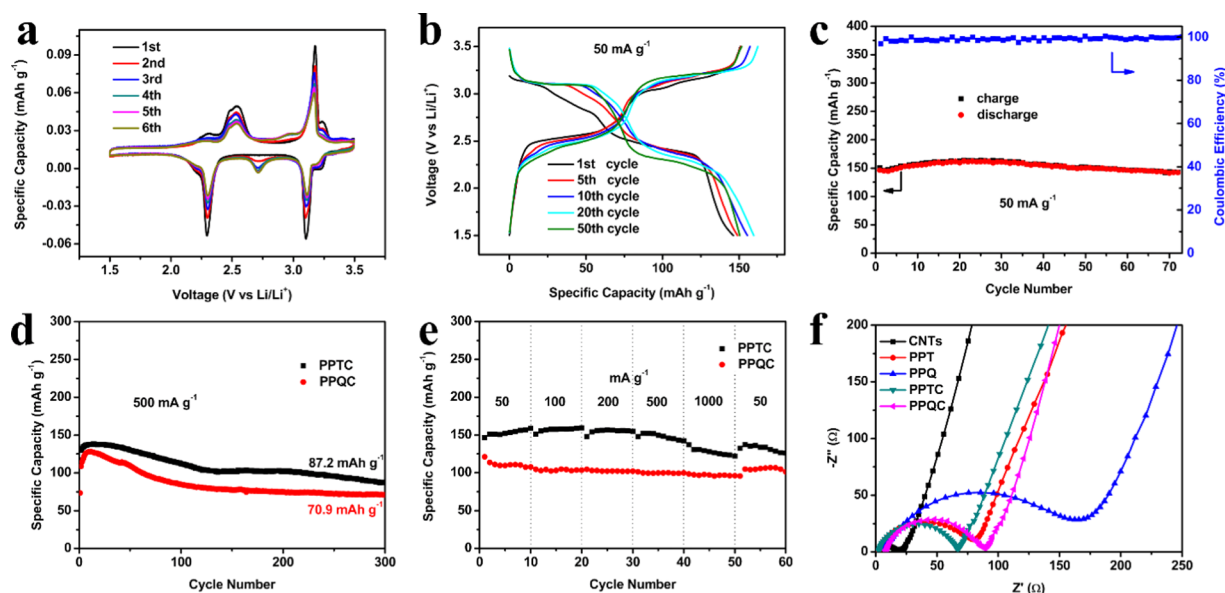


Figure 4. (a) CV curves of PPTC at 0.2 mV s^{-1} . (b) Galvanostatic discharge/charge curves and (c) cycling performance of PPTC at 50 mA g^{-1} . (d) Cycling performance at 500 mA g^{-1} and (e) rate performance at different current densities of PPTC and PPQC. (f) Nyquist plots of different samples.

contrast, the PPT shows a lower diffraction intensity, indicating the amorphous structure. Furthermore, the PPTC has similar peaks to those of PPT and CNTs, indicating the formation of hybrid films. Raman spectra is used to further investigate the chemical properties of the hybrid film (Figure 2c). Two typical peaks at 1340 cm^{-1} (D band) and 1581 cm^{-1} (G band) are observed, whose ratio (I_D/I_G) can be used to evaluate the disorder and graphitization degree of carbon materials.³⁶ Compared with the CNTs, the PPTC shows the increased intensity ratio of I_D/I_G , indicating the higher disorder degree and defect structure, which is in consistency with XRD patterns. The thermal stability of various samples is also characterized (Figure 2d). For PT, the first weight loss at $120 \text{ }^\circ\text{C}$ is attributed to the loss of solvent. Then, the structure is decomposed at $300 \text{ }^\circ\text{C}$ and the remained weight is $5.31 \text{ wt } \%$. For PPT, the decomposition of PPT takes place at $420 \text{ }^\circ\text{C}$ and the retained weight is $25.93 \text{ wt } \%$, which is attributed to the large planar ring of the PT unit and the extended rigid polymer chain.³² In contrast, the PPTC shows the highest remained weight of $82.17 \text{ wt } \%$ even at $1000 \text{ }^\circ\text{C}$. These results show that the hybrid films show superior thermal stability at elevated temperatures, which is beneficial for enhancing the safety as a cathode material for LIBs. In addition, the PPQ-based samples have also been characterized, which confirm the successful preparation of PPQC (Figures S7–S10).

The morphologies of various samples are investigated by scanning electron microscopy (SEM). It is obvious that the PT monomer shows a well-defined rectangular shape, while the PPT polymer shows irregular microparticles, suggesting their increased disorder degree after polymerization (Figure S11). Furthermore, the surface morphology of free-standing PPTC is investigated. As shown in Figure 3a, the CNT bundles tangle together to form an interconnected network with the smooth surface. In contrast, the PPTC film shows the morphology of long CNT-interconnected networks covered by PPT polymer particles (Figure 3b,c). When the concentration of the PPT polymer is increased, some PPT polymer particles can be clearly observed; however, when the concentration of the PPT

polymer is decreased, majority of CNT-interconnected networks can be clearly observed (Figure S12). Interestingly, the CNTs in the PPTC film could be served as the current collector. It is well known that the CNTs possess high electrical conductivity and mechanically robust; thus, the PPTC film can be directly served as a self-standing flexible electrode with good flexibility (Figure 3d). Furthermore, the dynamic mechanical analysis is used to examine the mechanical properties of the PPTC film. The stress–strain curves show that the tensile strength for the pure CNTs is 0.45 MPa with $3.7\% \text{ stain}$, while for the PPTC film, it is 1.97 MPa with $1.96\% \text{ stain}$ (Figure 3e). Their Young's moduli are calculated to be 0.012 and 0.101 GPa , respectively. The excellent mechanical performance shows exciting potential in organic-based bendable or wearable energy-storages devices.³⁰

The electrochemical performance of the samples is investigated as a working cathode for LIBs. Typically, cyclic voltammetry (CV) curves of samples are measured from 1.5 to 3.5 V (Figures 4a and S13). As observed, PT, PPT, and PPTC all show two main couples of redox peaks, which are attributed to two-stage successive lithiation/delithiation of the four carbonyl groups. In contrast, the redox potentials of PPT and PPTC are higher than those of PT ($3.07/3.25$ and $2.19/2.46 \text{ V}$ for PPT, $3.1/3.17$ and $2.29/2.54 \text{ V}$ for PPTC, and $2.95/3.2$ and $1.83/2.4 \text{ V}$ for PT), demonstrating that the extended conjugated structure can obviously enhance the redox potential.^{10,37,38} Also, PPTC shows higher redox potentials than those of PPQC, which is attributed to the multicarbonyl conjugated structure.¹⁰ In addition, PPTC shows additional two couples of weak redox peaks, which may be attributed to the greater utilization of redox-active sites resulting from the incorporation of the highly conductive CNTs.^{30,31} Interestingly, PPTC shows the almost overlapping CV profiles, indicating good reversibility. Figure 4b presents the galvanostatic discharge/charge (GDC) curves of PPTC at 50 mA g^{-1} . Due to the two-step lithiation/delithiation process of carbonyl groups, there are two discharge plateaus at 3.11 and 2.42 V and two charge plateaus at 3.22 and 2.56 V , which

tally with the CV curves. Also, PPTC exhibits high initial discharge capacity of 146.3 mAh g⁻¹. In addition, PPTC also shows high reversible discharge specific capacity of 142.5 mAh g⁻¹ with the Coulombic efficiency as high as ~100% after 70 cycles (Figure 4c). Remarkably, even at 500 mA g⁻¹, PPTC also shows high reversible discharge capacity of 87.2 mAh g⁻¹ with the capacity retention of 74.6% after 300 cycles (Figure 4d); the reduced capacity may result from the partly separation of active materials from CNTs. As a comparison, PPQC also shows high initial discharge capacity of 73.5 mAh g⁻¹ and has a discharge capacity of 70.9 mAh g⁻¹ after 300 cycles. It is obvious that PPQC shows lower discharge/charge capacities than those of PPTC, which can be easily understood in view of the increased number of the carbonyl groups. In fact, the different electrolytes also play a very crucial role in enhancing the electrochemical property of organic electrode materials, which has been confirmed by the reported literature works.³⁹ Also, the high addition of acetylene black could show higher capacities in the conventional electrode (Figure S14). In addition, the broad potential range of 1–3.5 V could also show higher capacities (Figure S15). Interestingly, PPT exhibits better electrochemical performance including a higher initial discharge capacity of 196.0 mAh g⁻¹ at 50 mA g⁻¹ and a reversible discharge capacity of 209.9 mAh g⁻¹ after 50 cycles compared with that of PT, which may be because the extension of the conjugated structure could increase the capacity and enhance the stability of organic electrode materials to a certain extent.^{39,40} At 200 mA g⁻¹, PPT can also deliver a high reversible capacity of 187.4 mAh g⁻¹ after 300 cycles (Figure S16a). Even at 1000 mA g⁻¹, the high capacity of 113.9 mAh g⁻¹ could also be maintained (Figure S16b). On the other hand, the content of the CNTs in the hybrid films is also examined. It is clear to find that PPTC exhibits the optimum cycling performance compared with that of PPTC-1 and PPTC-3 and the CNTs show negligible capacity contribution (Figure S17). Therefore, the active site utilization of PPT is affected by the electrical conductivity. During the electrochemical reactions, the active sites on the surface of the polymer may generate considerable capacity, but the active sites may be covered inside the inactive polymer, which may result in the low utilization of active site and release the low specific capacity.^{20,35,41} To study the influence of additional CNTs on fast discharge/charge processes, the rate performance of the PPTC and PPQC is shown in Figure 4e. PPTC shows superior rate capability to that of PPQC, including discharge capacities of 146.5, 151.3, 148.1, 148.1, and 137.1 mAh g⁻¹ at the current densities of 50, 100, 200, 500, and 1000 mA g⁻¹, respectively. When the current density returns to 50 mA g⁻¹, a high capacity of 132.5 mAh g⁻¹ can be recovered, indicating the faster reaction kinetics and excellent reversibility of PPTC and higher the energy density (Figure S18). To explain the reason for superior rate capability of PPTC, electrochemical impedance spectroscopy is measured (Figure 4f). The semicircles in the high-frequency region represent the R_{ct} between the electrode materials and the electrolyte interface, which corresponds to the reaction kinetics of electrode materials.²¹ Obviously, the hybrid films show smaller R_{ct} values than those of polymers, which could be because the incorporation of CNTs increases the conductivity. In addition, the R_{ct} of PPT-based cathode materials is smaller than that of PPQ-based cathode materials, which could be because the extension of the conjugated structure can increase the conductivity of organic electrode materials to a certain

extent.³⁸ Based on these excellent features, the PPTC shows comparable electrochemical performance to that of the reported organic cathodes (Table S1).

To study the structure change of PPT during the Li⁺ intercalation/deintercalation process, ex situ FT-IR spectra are measured. The characteristic peaks at around 1666 cm⁻¹ for carbonyl groups become weaker after the first discharge process and then recover as the following charge process, indicating the reversible reaction of the carbonyl groups (Figure S19). In addition, a similar phenomenon can also be observed after the 10th discharge/charge process, indicating the good stability and excellent redox activity of PPT. According to the analyses above, the reaction mechanism of the PT unit can be supposed to be of two steps for the storage of four Li⁺ ions (Figure 5a). During the discharge process, two

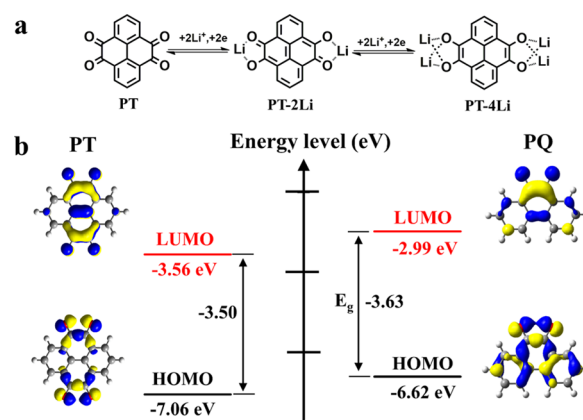


Figure 5. (a) Electrochemical reaction mechanism of the PT unit. (b) HOMO/LUMO energy levels and orbit distribution of PT and PQ.

Li⁺ ions are first captured by the carbonyl groups of PT, thus forming symmetrical lithiated PT-2Li. Then, another two Li⁺ ions are further captured to form PT-4Li. After the following charge process, the Li⁺ ions separate from the carbonyl groups and the PT unit with four carbonyl groups could be recovered. The symmetry structure of PT may improve the chemical stability and decrease the polarization effect during the redox reaction, which can effectively improve the electrochemical performance.¹⁰ To provide deeper insight into the different electrochemical properties of PPT and PPQ, the energy levels of highest occupied molecular orbital (HOMO) and the lowest unoccupied molecular orbital (LUMO) for the PT and PQ are calculated by density functional theory (DFT).^{28,42} According to the molecular orbital theory, a molecule with a lower LUMO energy level always has greater electron affinity and better oxidizability, thus showing a higher reduction potential. In contrast, PT shows a lower LUMO energy level (−3.56 eV) than that of PQ (−2.99 eV) (Figure 5b), which confirms that extending the conjugated structure of the molecule could lower its LUMO energy level, thus showing greater electron affinity and higher reduction potential.^{10,37,43} This result is in agreement with the CV curves of PPTC and PPQC (Figures 4a and S13). In addition, the energy gap (E_g) between HOMO and LUMO energy levels can be used to indicate the electronic conduction. In contrast, PT shows smaller E_g value (−3.50 eV) than that of PQ (−3.63 eV), which confirms that extending the conjugated structure of molecule could narrow its energy gap, thus showing higher electronic conduction. This result is in agreement with the rate performance of PPTC and PPQC

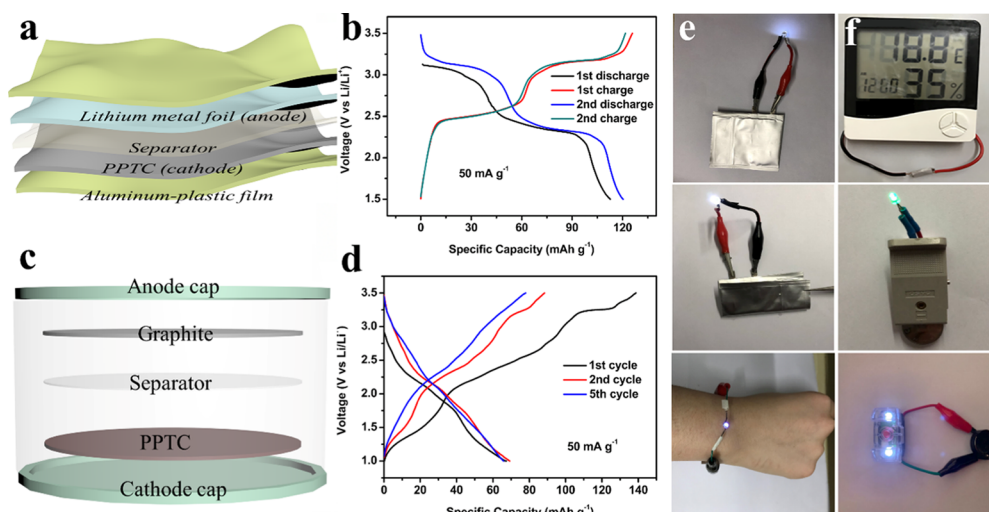


Figure 6. (a) Schematic representation and (b) discharge/charge curves of the flexible battery. (c) Schematic representation and (d) discharge/charge curves of the full cell. Digital photographs of LED lighting by the flexible battery under different conditions (e) and lighting of different devices by the full cell (f).

(Figure 4e). In addition, the PT also exhibits a much smaller E_g compared to the larger E_g for most of the organic electrodes (4.16 eV for 9,10-anthraquinone and 3.76 eV for 1,4-benzoquinone) in previous literature works.⁴⁴ After capturing Li^+ ions, the E_g values of $\text{PT-}x\text{Li}$ ($x = 2$ or 4) are further decreased (2.91 eV for $\text{PT-}2\text{Li}$ and 2.40 eV for $\text{PT-}4\text{Li}$, Figure S20), indicating the increasing chemical reactivity of $\text{PT-}x\text{Li}$. Moreover, the extended conjugation can decrease the E_g value and reduce the degree of polarization; thus, the PPTs may exhibit excellent electrochemical performance as a cathode material for LIBs.³⁷ Furthermore, it is clearly seen that the HOMO and LUMO orbits of all of the samples are mainly distributed on their benzene ring, which may be attributed to the effective conjugation between the aromatic ring and the carbonyl groups.¹⁰ The above results demonstrate that the stable and symmetrical conjugated structure of the PT unit can promote the combination with four Li^+ ions during the electrochemical reaction.

To demonstrate the practical application of the PPTC flexible electrode, the flexible battery and the full cell are assembled. In Figure 6a, the PPTC flexible cathode is paired up with the lithium foil to form the flexible battery. Interestingly, the PPTC-based flexible battery can exhibit high initial discharge/charge capacities of 112.7/125.8 mAh g^{-1} at 50 mA g^{-1} (Figure 6b). Furthermore, the full cell has been assembled through coupling PPTC with graphite (Figure 6c). In Figure 6d, the typical GDC curves show that the full cell can exhibit the initial charge/discharge capacities of 138.7/72.8 mAh g^{-1} (calculated based on the mass of PPTC). Certainly, the electrochemical performance of the full cell should be improved by adjusting the electrolyte, preactivating the electrode, or changing the mass ratio of the cathode with anode. As a proof of concept, an light-emitting diode (LED) can be easily lighted by a flexible battery, even when the battery is bended or processed into a simple bracelet (Figure 6e), and the full cell can power various devices, including an electronic thermometer, an LED, and a small bike lamp (Figure 6f).

4. CONCLUSIONS

In summary, we have synthesized a series of conjugated carbonyl polymers including PT and PQ units using the coupling polymerization reaction and constructed flexible, binder-free, and free-standing PPTC and PPQC cathodes for LIBs. The methodology not only inhibits the dissolution of monomer and extends the conjugated structure of molecule but also enhances the electronic conductivity of organic materials and endows the electrode with flexible features. When used as a flexible cathode for LIBs, the PPTC exhibits higher discharge plateau, good Li^+ storage property, and excellent rate capability. Furthermore, the reaction mechanism of the conjugated carbonyl polymers is also elucidated by experimental and theoretical analyses, which demonstrate that the multicarbonyl and symmetrical conjugated structure of the PT unit is beneficial to improving the electrochemical performance. Therefore, the present strategy using the coupling polymerization reaction and vacuum-filtration method may open up a new avenue for constructing a conjugated carbonyl polymer-based flexible electrode with high performance for application in bendable or wearable energy-storage devices.

■ ASSOCIATED CONTENT

Supporting Information

The Supporting Information is available free of charge on the ACS Publications website at DOI: 10.1021/acsami.9b06437.

Synthetic procedure of PT, PT-2Br, PQ-2Br and PPQ; ^1H NMR data; UV-vis spectra; solubility test; detailed characterization of PPQC; SEM images; corresponding electrochemical tests; summary of the electrochemical properties of organic electrode materials; ex situ FT-IR spectra; and theoretical analyses (PDF)

■ AUTHOR INFORMATION

Corresponding Authors

*E-mail: wanghengguo@cust.edu.cn (H.-g.W.).

*E-mail: szj@cust.edu.cn (Z.S.).

*E-mail: duanqian88@hotmail.com (Q.D.).

ORCID 

Zhenjun Si: 0000-0001-9365-6567

Notes

The authors declare no competing financial interest.

ACKNOWLEDGMENTS

This work was financially supported by the Science & Technology Department of Jilin Province (No. 20170101177JC).

REFERENCES

- (1) Armand, M.; Tarascon, J. M. Building Better Batteries. *Nature* **2008**, *451*, 652–657.
- (2) Lewis, N. S. Research Opportunities to Advance Solar Energy Utilization. *Science* **2016**, *351*, aad1920.
- (3) Etacheri, V.; Marom, R.; Elazari, R.; Salitra, G.; Aurbach, D. Challenges in the Development of Advanced Li-ion Batteries: A Review. *Energy Environ. Sci.* **2011**, *4*, 3243–3262.
- (4) Muench, S.; Wild, A.; Friebe, C.; Häupler, B.; Janoschka, T.; Schubert, U. S. Polymer-based Organic Batteries. *Chem. Rev.* **2016**, *116*, 9438–9484.
- (5) Liang, Y.; Tao, Z.; Chen, J. Organic Electrode Materials for Rechargeable Lithium Batteries. *Adv. Energy Mater.* **2012**, *2*, 742–769.
- (6) Song, Z.; Zhou, H. Towards Sustainable and Versatile Energy Storage Devices: An Overview of Organic Electrode Materials. *Energy Environ. Sci.* **2013**, *6*, 2280–2301.
- (7) Visco, S. J.; Mailhe, C. C.; Jonghe, L. C. D.; Armand, M. B. A Novel Class of Organosulfur Electrodes for Energy Storage. *J. Electrochem. Soc.* **1989**, *136*, 661–664.
- (8) Suga, T.; Konishi, H.; Nishide, H. Photocrosslinked Nitroxide Polymer Cathode-Active Materials for Application in an Organic-based Paper Battery. *Chem. Commun.* **2007**, 1730–1732.
- (9) Kim, Y.; Jo, C.; Lee, J.; Lee, C. W.; Yoon, S. An Ordered Nanocomposite of Organic Radical Polymer and Mesocellular Carbon Foam as Cathode Material in Lithium ion Batteries. *J. Mater. Chem.* **2012**, *22*, 1453–1458.
- (10) Liang, Y. L.; Zhang, P.; Chen, J. Function-Oriented Design of Conjugated Carbonyl Compound Electrodes for High Energy Lithium Batteries. *Chem. Sci.* **2013**, *4*, 1330–1337.
- (11) Wang, H. G.; Yuan, S.; Ma, D. L.; Huang, X. L.; Meng, F. L.; Zhang, X. B. Tailored Aromatic Carbonyl Derivative Polyimides for High-Power and Long-Cycle Sodium-Organic Batteries. *Adv. Energy Mater.* **2014**, *4*, No. 1301651.
- (12) Genorio, B.; Pirnat, K.; Cerc-Korosec, R.; Dominko, R.; Gaberscek, M. Electroactive Organic Molecules Immobilized onto Solid Nanoparticles as a Cathode Material for Lithium-Ion Batteries. *Angew. Chem., Int. Ed.* **2010**, *49*, 7222–7224.
- (13) Song, C. K.; Eckstein, B. J.; Tam, T. L. D.; Trahey, L.; Marks, T. J. Conjugated Polymer Energy Level Shifts in Lithium-Ion Battery Electrolytes. *ACS Appl. Mater. Interfaces* **2014**, *6*, 19347–19354.
- (14) Wu, H.; Yu, G.; Pan, L.; Liu, N.; McDowell, M. T.; Bao, Z.; Cui, Y. Stable Li-ion Battery Anodes by In-Situ Polymerization of Conducting Hydrogel to Conformally Coat Silicon Nanoparticles. *Nat. Commun.* **2013**, *4*, No. 1943.
- (15) Ma, T.; Zhao, Q.; Wang, J.; Pan, Z.; Chen, J. A Sulfur Heterocyclic Quinone Cathode and a Multifunctional Binder for a High-Performance Rechargeable Lithium-Ion Battery. *Angew. Chem.* **2016**, *128*, 6538–6542.
- (16) Kim, K. C.; Liu, T. Y.; Lee, S. W.; Jang, S. S. First-Principles Density Functional Theory Modeling of Li Binding: Thermodynamics and Redox Properties of Quinone Derivatives for Lithium-Ion Batteries. *J. Am. Chem. Soc.* **2016**, *138*, 2374–2382.
- (17) Shin, D. S.; Park, M.; Ryu, J.; Hwang, I.; Seo, J. K.; Seo, K.; Cho, J.; Hong, S. Y. Nonaqueous Arylated Quinone Catholytes for Lithium-Organic Flow Batteries. *J. Mater. Chem. A* **2018**, *6*, 14761–14768.
- (18) Yuan, C. P.; Wu, Q.; Li, Q.; Duan, Q.; Li, Y. H.; Wang, H. G. Nanoengineered Ultralight Organic Cathode Based on Aromatic Carbonyl Compound/Graphene Aerogel for Green Lithium and Sodium Ion Batteries. *ACS Sustainable Chem. Eng.* **2018**, *6*, 8392–8399.
- (19) Yuan, C. P.; Wu, Q.; Shao, Q.; Li, Q.; Gao, B.; Duan, Q.; Wang, H. G. Free-Standing and Flexible Organic Cathode based on Aromatic Carbonyl Compound/carbon nanotube Composite for Lithium and Sodium Organic Batteries. *J. Colloid Interface Sci.* **2018**, *517*, 72–79.
- (20) Geng, J.; Bonnet, J. P.; Renault, S.; Dolhem, F.; Poizot, P. Evaluation of Polyketones with Ncyclic Structure as Electrode Material for Electrochemical Energy Storage: Case of Tetraketopiperazine Unit. *Energy Environ. Sci.* **2010**, *3*, 1929–1933.
- (21) Chen, H.; Armand, M.; Demailly, G.; Dolhem, F.; Poizot, P.; Tarascon, J. M. From Biomass to a Renewable LiXC₆O₆ Organic Electrode for Sustainable Li-Ion Batteries. *ChemSusChem* **2008**, *1*, 348–355.
- (22) Yokoji, T.; Matsubara, H.; Satoh, M. Rechargeable Organic Lithium-ion Batteries using Electron-Deficient Benzoquinones as Positive-Electrode Materials with High Discharge Voltages. *J. Mater. Chem. A* **2014**, *2*, 19347–19354.
- (23) Wang, Y.; Liu, Z.; Liu, H.; Li, B.; Guan, S. A Novel High-Capacity Anode Material Derived from Aromatic Imides for Lithium-Ion Batteries. *Small* **2018**, *14*, No. 1704094.
- (24) Ahmad, A.; Meng, Q. H.; Melhi, S.; Mao, L. J.; Zhang, M.; Han, B. H.; Lu, K.; Wei, Z. X. A Hierarchically Porous Hypercrosslinked and Novel Quinone based Stable Organic Polymer Electrode for Lithium-Ion Batteries. *Electrochim. Acta* **2017**, *255*, 145–152.
- (25) Zhao, Q.; Wang, J.; Chen, C.; Ma, T.; Chen, J. Nanostructured Organic Electrode Materials Grown on Graphene with Covalent-bond Interaction for High-Rate and Ultra-Long-Life Lithium-Ion Batteries. *Nano Res.* **2017**, *10*, 4245–4255.
- (26) Zhu, Z. Q.; Hong, M. L.; Guo, D. S.; Shi, J. F.; Tao, Z. L.; Chen, J. All-Solid-State Lithium Organic Battery with Composite Polymer Electrolyte and Pillar [5] Quinone Cathode. *J. Am. Chem. Soc.* **2014**, *136*, 16461–16464.
- (27) Mukherjee, D.; Gowda, Y. K. G.; Kotresh, H. M. N.; Sampath, S. Porous, Hyper-Cross-Linked, Three-Dimensional Polymer as Stable, High Rate Capability Electrode for Lithium-Ion Battery. *ACS Appl. Mater. Interfaces* **2017**, *9*, 19446–19454.
- (28) Milton, R. D.; Hickey, D. P.; Abdellaoui, S.; Lim, K.; Wu, F.; Tan, B. X.; Minter, S. D. Rational Design of Quinones for High Power Density Biofuel Cells. *Chem. Sci.* **2015**, *6*, 4867–4875.
- (29) Letizia, J. A.; Cronin, S.; Ortiz, R. P.; Facchetti, A.; Ratner, M. A.; Marks, T. J. Phenacyl-Thiophene and Quinone Semiconductors Designed for Solution Processability and Air-Stability in High Mobility n-Channel Field-Effect Transistors. *Chem. - Eur. J.* **2010**, *16*, 1911–1928.
- (30) Amin, K.; Meng, Q. H.; Ahmad, A.; Cheng, M.; Zhang, M.; Mao, L. J.; Lu, K.; Wei, Z. X. A Carbonyl Compound-Based Flexible Cathode with Superior Rate Performance and Cyclic Stability for Flexible Lithium-Ion Batteries. *Adv. Mater.* **2018**, *30*, No. 1703868.
- (31) Lu, Y.; Zhao, Q.; Miao, L.; Tao, Z.; Niu, Z.; Chen, J. Flexible and Free-Standing Organic/Carbon Nanotubes Hybrid Films as Cathode for Rechargeable Lithium-Ion Batteries. *J. Phys. Chem. C* **2017**, *121*, 14498.
- (32) Yamamoto, T.; Etori, H. Poly(anthraquinone)s Having a π -Conjugation System along the Main Chain. Synthesis by Organometallic Polycondensation, Redox Behavior, and Optical Properties. *Macromolecules* **1995**, *28*, 3371–3379.
- (33) Song, Z. P.; Qian, Y. M.; Gordin, M. L.; Tang, D. H.; Xu, T.; Otani, M.; Zhan, H.; Zhou, H. S.; Wang, D. H. Polyanthraquinone as a Reliable Organic Electrode for Stable and Fast Lithium Storage. *Angew. Chem., Int. Ed.* **2015**, *54*, 13947.
- (34) Yamamoto, T. π -Conjugated Polymers with Electronic and Optical Functionalities: Preparation by Organometallic Polycondensation, Properties, and Applications. *Macromol. Rapid Commun.* **2002**, *23*, 583–606.

(35) Pirnat, K.; Bitenc, J.; Vizintin, A.; Krajnc, A.; Tchernychova, E. Indirect Synthesis Route toward Cross-Coupled Polymers for High Voltage Organic Positive Electrodes. *Chem. Mater.* **2018**, *30*, 5726–5732.

(36) Jiang, C.; Yuan, C.; Li, P.; Wang, H. G.; Li, Y. H.; Duan, Q. Nitrogen-Doped Porous Graphene with Surface Decorated MnO₂ Nanowires as a High-Performance Anode Material for Lithium-Ion Batteries. *J. Mater. Chem. A* **2016**, *4*, 7251–7256.

(37) Banda, H.; Damien, D.; Nagarajan, K.; Raj, A.; Hariharan, M.; Shaijumon, M. Twisted Perylene Diimides with Tunable Redox Properties for Organic Sodium-Ion Batteries. *Adv. Energy Mater.* **2017**, *7*, No. 170136.

(38) Wang, C. L.; Xu, Y.; Fang, Y. G.; Zhou, M.; Liang, L. Y.; Singh, S.; Zhao, H. P.; Schober, A.; Lei, Yong. Extended π -Conjugated System for Fast-Charge and -Discharge Sodium-Ion Batteries. *J. Am. Chem. Soc.* **2015**, *137*, 3124–3130.

(39) Kurimoto, N.; Omoda, R.; Mizumo, T.; Ito, S.; Aihara, Y.; Itoh, T. Four-Electron Transfer Tandem Tetracyanoquinodimethane for Cathode-active Material in Lithium Secondary Battery. *J. Power Sources* **2018**, *377*, 12–17.

(40) Huang, Y.; Li, K.; Liu, J.; Zhong, X.; Duan, X.; Shakir, I.; Xu, Y. Three-Dimensional Graphene/Polyimide Composite-Derived Flexible High-Performance Organic Cathode for Rechargeable Lithium and Sodium Batteries. *J. Mater. Chem. A* **2017**, *5*, 2710–2716.

(41) Zhao, L. B.; Gao, S. T.; He, R. X.; Shen, W.; Li, M. Electronic Structure Oriented Molecular Design of Phenanthrenequinone Derivatives for Organic Cathode Materials. *ChemSusChem* **2018**, *11*, 1215–1222.

(42) Song, Z. P.; Zhan, H.; Zhou, Y. H. Polyimides: Promising Energy-Storage Materials. *Angew. Chem., Int. Ed.* **2010**, *49*, 8444–8448.

(43) Lee, J.; Kim, H.; Park, M. J. Long-Life, High-Rate Lithium-Organic Batteries Based on Naphthoquinone Derivatives. *Chem. Mater.* **2016**, *28*, 2408–2416.

(44) Xie, J.; Zuo, T. F.; Huang, Z. L.; Huan, L.; Gu, Q. X.; Gao, C. X.; Shao, J. J. Theoretical Study of a Novel Imino Bridged Pillar[5]arene Derivative. *Chem. Phys. Lett.* **2016**, *662*, 25–30.